Ranta, Janne; Polojärvi, Arttu; Tuhkuri, Jukka

Sources of Stochasticity in Ice-Structure Interaction Process

Published in:
Proceedings of the 24th International Conference on Port and Ocean Engineering under Arctic Conditions, POAC'17

Published: 01/01/2017

Document Version
Publisher's PDF, also known as Version of record

Please cite the original version:
Ranta, J., Polojärvi, A., & Tuhkuri, J. (2017). Sources of Stochasticity in Ice-Structure Interaction Process. In Proceedings of the 24th International Conference on Port and Ocean Engineering under Arctic Conditions, POAC'17 (Proceedings : International Conference on Port and Ocean Engineering Under Arctic Conditions). POAC.

POAC'17
Busan, KOREA

Proceedings of the 24th International Conference on
Port and Ocean Engineering under Arctic Conditions
June 11-16, 2017, Busan, Korea

Sources of Stochasticity in Ice-Structure Interaction Process

Janne Ranta[1,2], Arttu Polojärvi[1,2] and Jukka Tuhkuri[1,2]

[1]Aalto University, School of Engineering, Department of Mechanical Engineering P.O. Box 14300, FI-00076 Aalto, Finland
[2]Sustainable Arctic Marine and Coastal Technology (SAMCoT), Centre for Research-based Innovation (CRI), Norwegian University of Science and Technology, Trondheim, Norway

ABSTRACT

We simulated the ice-structure interaction process using 2D FEM-DEM. The simulations are deterministic, but sensitive to initial conditions. Ice loads statistics from three sets of 50 simulations were considered. The sets differed by ice crushing strength. In two set the ice sheet was homogeneous and in one set the crushing strength of ice varied. In simulations with homogeneous ice sheets the initial condition varied causing different load records. In the case of the non-homogenous ice sheets, variation in load records came directly through the non-homogeneity of the sheet. Our core result is that the stochastic nature of ice loads could be due to the non-homogeneity of sea ice, but virtually as much variation in the data was observed with homogenous ice sheets. This suggests that the variability in the ice loads was mainly caused by the ice-structure interaction process instead of the non-homogeneity of ice.

INTRODUCTION

Arctic marine operations increase continuously. This includes developments in Northern sea transportation, offshore drilling operations, and offshore wind energy. One of the key factors in developing safe Arctic operations is a reliable prediction of sea ice loads, which are induced by ice-structure interaction process. Here we focus on on the statistics of the ice loads induced by an ice-inclined structure interaction processes by studying these processes using 2D combined finite-discrete element method simulations (2D FEM-DEM). We investigate where the well- known stochastic nature of ice loads (Daley et al., 1998; Jordaan, 2001) arises from. Often this stochasticity is assumed to be due to the inhomogeneity of ice.

Our 2D FEM-DEM simulations of the ice-structure interaction process are deterministic, but we know that the process is very sensitive to its initial conditions (Ranta et al., 2017a). Here we used this sensitivity to create sets of simulations using the same simulation parameters, but different initial conditions. For a set of simulations, we conducted 50 simulations with constant parameters, but varying vertical initial velocity v_0 at the free end of the ice sheet (see Figure 1). This v_0 was given a random value of the order of 10^{-9} mms^{-1}. This was enough to cause different ice failure processes. After this we ran one more set of 50 simulations where the ice

sheet was non-homogenous. This gave us data on the processes in the case of non-homogenous ice (vertical initial velocity v_0 was zero in these simulations).

The core finding here is that, the stochastic nature of ice loads could be due to non-homogeneity of sea ice, but it can as well simply arise from the ice-structure interaction process itself. The

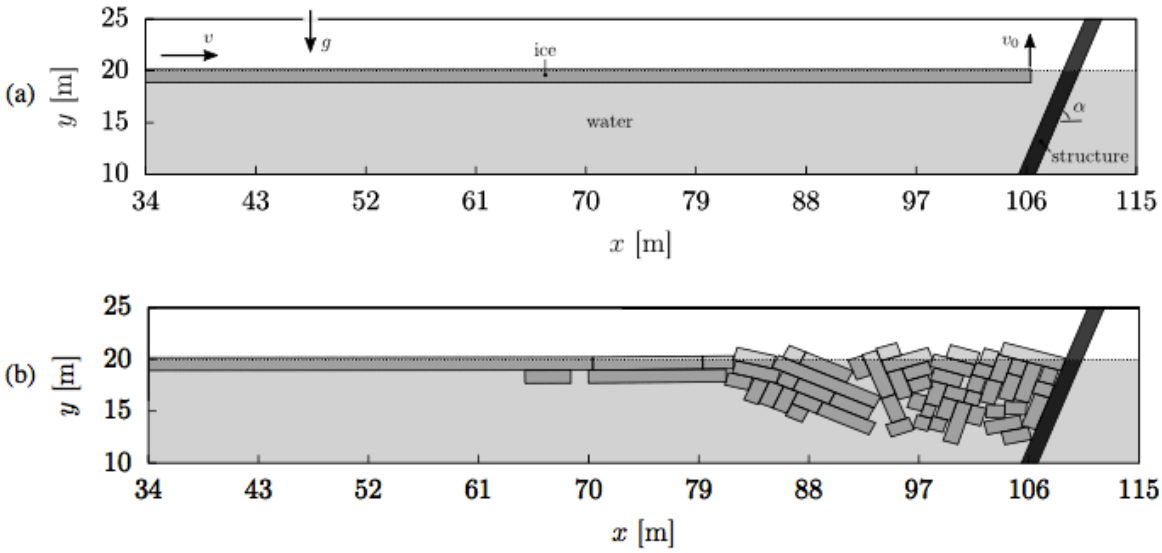

Figure 1: (a) Simulation set-up: A floating ice sheet (dark grey) is pushed with a velocity of v = 50 mms^{-1} towards an inclined (α = 70°) structure (black). The water is colored light gray. A perturbation for the initial conditions was created by giving a low vertical velocity v_0 for the free end of the ice sheet. v_0 was of the order of 10^{-9} mms^{-1} and varied randomly between all simulations. (b) A snapshot from a simulation at a stage where the length of the pushed ice L = 125 m. Ice thickness h = 1.25 m and plastic limit σ_p = 1 MPa.

ice-structure interaction process is itself a stochastic process. We will first describe the simulation tools. After this we present our results, and analyze and discuss them. We look into the peak load statistics and compare the processes that have homogenous ice sheets to those which have a non-homogenous sheets. We conclude the paper with some remarks on our work.

SIMULATIONS

The 2D FEM-DEM simulation tools we used are the same as used in Paavilainen et al. (2009, 2011), Paavilainen and Tuhkuri (2012, 2013), and Ranta et al. (2017a). We use the 2D FEM-DEM code of Aalto University Ice Mechanics Group. The DEM part of the code follows the model by Hopkins (1992) while Paavilainen et al. (2009) developed the FEM-DEM Timoshenko beam model for the ice sheet. The model was validated in Paavilainen et al. (2009, 2011) against laboratory and full-scale measurements on ice loads. Polojärvi et al. (2015) successfully used the DEM part for modeling direct shear box tests on ice rubble.

Figure 1 illustrates the simulations. We have a floating, homogenous and continuous ice sheet pushed against an inclined rigid structure with constant velocity v. The initially intact ice sheet breaks into ice blocks, which then interact with each other and the structure. Modeling of the

ice-structure interaction process requires a numerical model, where the formation of the rubble pile and its interaction with both, the advancing ice sheet and the structure, are accounted for. Table 1 lists the simulation parameters, which we mostly chose after Timco and Weeks (2010).

We ran three sets S1, S2 and S3 of 50 simulations summarized in Table 2. Within sets S1 and S2, all parameters, except the initial velocity perturbation v_0, were constant. These simulation sets had a different value for the ice plastic limit σ_p in contact. Plastic limit σ_p describes the local ice crushing in contacts, but the model is not able to describe the continuous crushing of intact ice nor the extrusion of crushed ice. The simulations of set S3 were ran with a non-homogeneous ice sheet. In these simulations σ_p randomly varied between values 1 and 2 MPa within the sheet. All of the ice sheets of the simulations in S3 were unique, with σ_p varying after uniform distribution throughout the sheet. This was done by giving each discrete element of the ice sheet a random σ_p value. Simulations of S3 did not have an initial velocity perturbation; The potential stochasticity in the results of simulations in S3 thus arises from the non-homogeneity of the modeled ice.

Figures 2a and b illustrate how the initial velocity perturbation affects the load records from the ice failure process in simulations of set S1. Here F is plotted as a function of L, the length of the ice sheet pushed against the structure. The load records show similar features, but they diverge after the first load peaks at around $L = 10 \ldots 15$ m. Figure 2b shows the maximum ice loads F^p event for both of the simulations in Figure 2b. The F records between the simulated processes differ, which causes the values of F^p and L at their occurrence to differ. Simulations of sets S2 and S3 yielded similar load records, and the discussion of this paragraph applies for them as well.

Table 1: Summary of the main simulation parameters used in the 300 simulations of this paper. Ice thickness h and plastic limit σ_p were varied. Other parameters had the values given by the table in all simulations. The parameter values were mostly chosen after Timco and Weeks (2010).

	Description and symbol		Unit	Value or Range
General	Gravitational acceleration	g	m/s^2	9.81
	Ice Sheet velocity	v	m/s	0.05
	Drag coefficient	c_d		2.0
Ice	Thickness	h	m	1.25
	Effective modulus	E	GPa	4
	Poisson's ratio	ν		0.3
	Density	ρ_i	kg/m^3	900
	Tensile strength	σ_f	MPa	0.6
	Shear strength	τ_f	MPa	0.6
Contact	Plastic limit	σ_P	MPa	1.0-2.0
	Ice-ice friction coefficient	μ_{ii}		0.1
	Ice-structure friction coefficient	μ_{iw}		0.1
Water	Density	ρ_w	kg/m^3	1010
Structure	Slope angle	α	deg	70

Table 2: Summary of simulations sets S1-S3. Sets differed of simulations was 150. by the values of σ_p. Total number

Set	IDs	n	h	σ_P
			[m]	[MPa]
S1	1-50	50	1.25	1
S2	51-100	50	1.25	2
S3	101-150	50	1.25	$U(1,2)$

The data analyzed here consisted of above-described three sets of 50 simulations. If data from the 50 simulations were combined into a single graph, we would get a similar graph as in Figure 2a for 2 simulations, but such a graph would not be informative. Since we have 50 load values for each time step from the 50 simulations in each set, we could calculate the mean ice load, standard deviation and maximum load for each time step. Figure 3 illustrates how these statistical measures for a given time step were obtained from the load records. In this way we define the mean load, standard deviation of the load, and the maximum load for each time step.

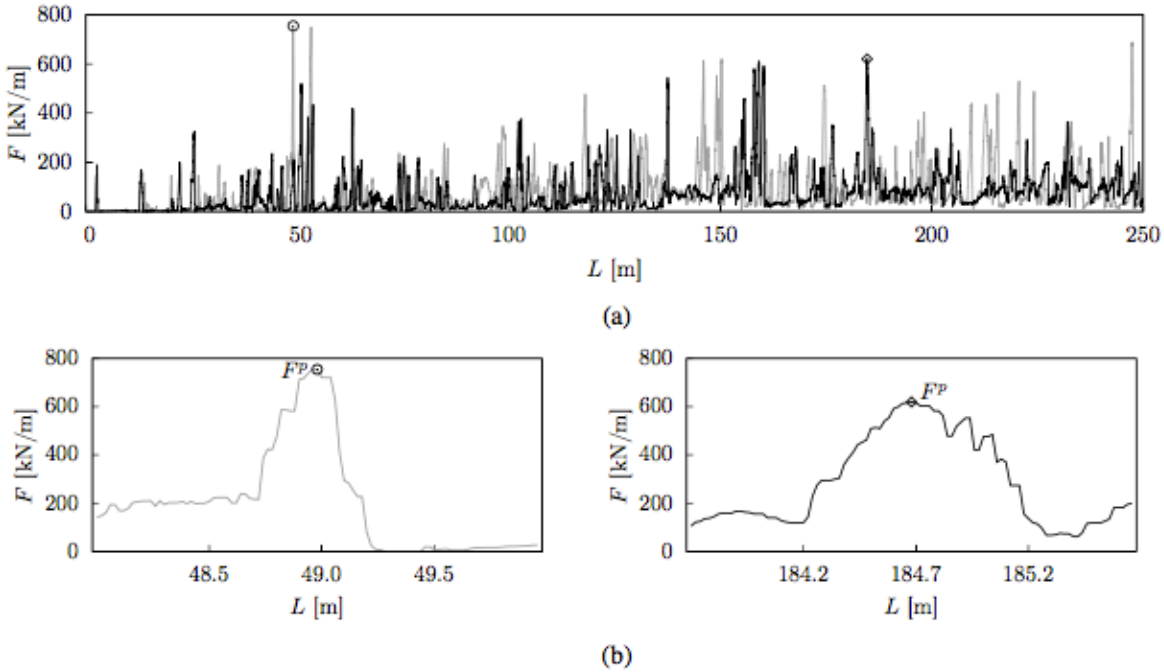

Figure 2: Two ice load F records from simulations of set S1: (a) F plotted against length L of pushed ice and (b) two close-ups of the peak ice load F_p events from the same two simulations. The F records diverged after the L = 10 . . . 15 meters of pushed ice.

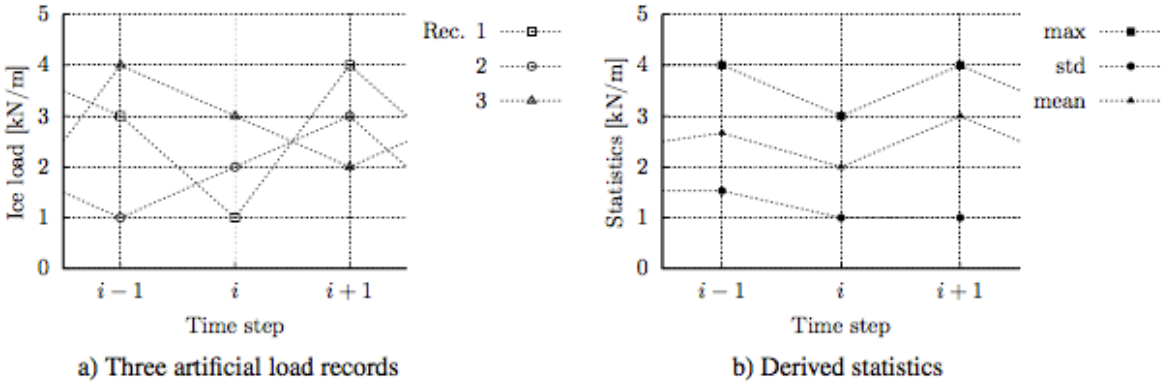

Figure 3: Illustration on how the mean (mean), standard deviation (std) and maximum (max) ice load records were obtained: (a) Data from three time steps $i-1$, i and $i+1$ from three artificial load records. (b) The derived statistics for these time steps.

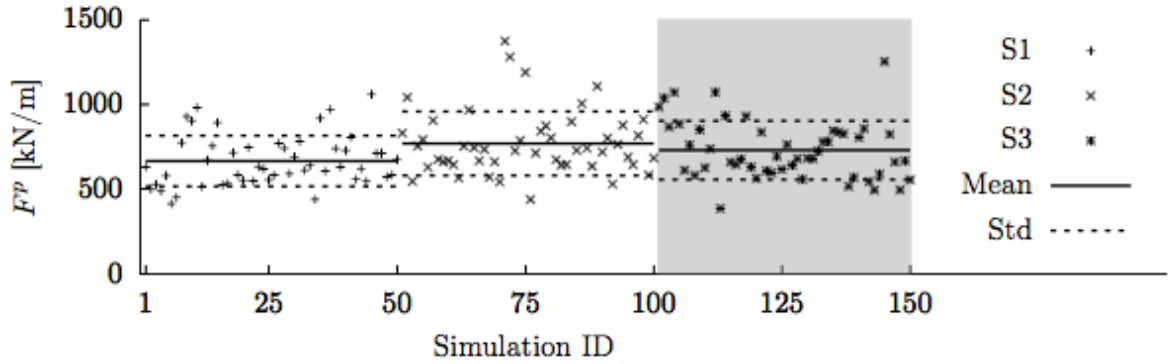

Figure 4: Peak ice load observations from simulation sets 1–3. Solid horizontal lines indicate set mean values and dashed lines are ± one standard deviation away from the mean. Results from set 3 with non-homogenous ice sheets are highlighted by gray background color.

RESULTS AND ANALYSIS

Figure 4 shows global peak ice load F_P values from all simulations used in the analysis. In the figure, the horizontal axis indicates the simulation ID and the vertical axis shows F_P value for each observation. In addition, the figure shows the mean values and standard deviations for the data points belonging to each set S1-S3. These mean values and the standard deviations are also summarized in Table 3, which additionally gives the coefficient of variation c_v (the standard deviation of a set divided by the corresponding mean value) values for all sets. Value of c_v describes the variability in the underlying data set.

As seen from Figure 4, the data points from the different sets fall onto same regime. The mean F_P value for S2 (for which σ_p = 2 MPa) is slightly higher than for S1 (σ_p = 1 MPa), and the mean value for S3 falls between the means of sets S1 and S2. The figure together with the standard deviations of Table 3 indicate, the data set pair S1 and S3 are very similar. Same applies to pair S2 and S3. The similarity in the data sets is also indicated by the values of the c_v, also given in the table. They all are about equal. These statistical figures do not allow us to

distinguish the data set yielded by the simulations with non-homogenous ice sheet from those yielded by homogenous sheet.

In addition to these features, also the distributions of the peak load data were very similar as shown by Figures 5a and b. The figures, respectively, show the relative frequencies of the peak load F_P observations, sorted here into 10 equally sized bins, and the empirical cumulative distribution functions for F_P values. The figures show that the distributions for sets S1-S3 clearly follow very similar trends, and in fact, the histograms of Figure 5a are even difficult to tell apart. We did not attempt to look for the best fitting distribution for the data sets in the histogram of Figures 5a, but the shape of the histogram indicates them to be non-normal (Ranta et al., 2017b).

Table 3: The mean of global peak loads F_P values, their standard deviations (std), and the coefficients of variation (c_v) for the simulations of all sets S1-S3.

Set	Mean(F^P)[kN/m]	std(F^P)[kN/m]	c_v[-]
S1	670	150	0.22
S2	770	190	0.25
S3	730	170	0.23

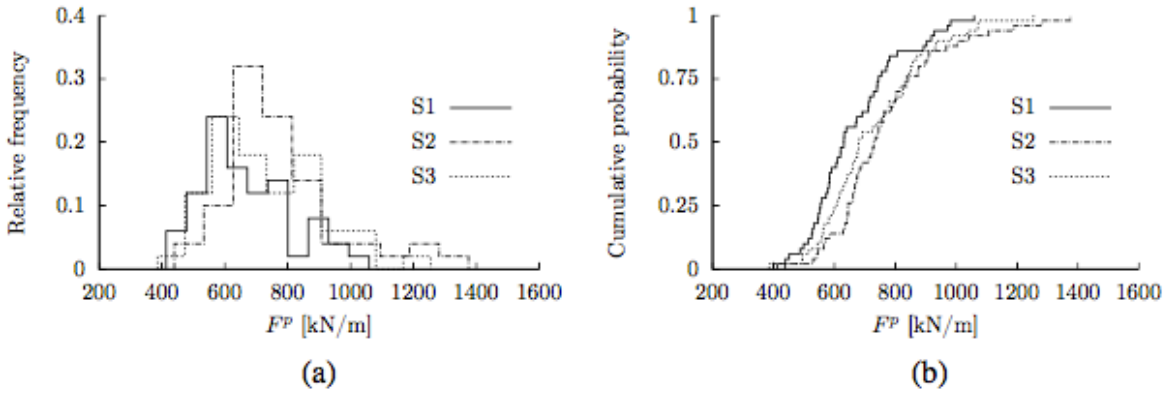

Figure 5: Relative frequencies (a) of peak loads from simulation data sets 1–3 and empirical cumulative distribution functions (b) of the same data sets.

We can also compare the so-called concurrent statistical values from the different processes, that is, the statistics of load F values from the same time step of the different simulations. The derivation of these time-step-wise statistical figures was described above (see Figure 3). Figures 6a-c show comparisons for the mean load, for the standard deviation, and for the maximum load, respectively. Left column of the figure depicts comparisons of loads between simulation S1 and S3 and the right column between simulation sets S2 and S3. The x- and y-coordinates of each data point are, respectively, defined by the value of a given statistical figure from the sets S1-S3 given as the label of x- and y-axis. If the data sets matched one-to-one, all of the data points would fall on the diagonal also shown in the plots.

Figures 6a-c illustrate that the concurrent load values from the different sets of 50 simulations do not show any dependency of the set: all of the point clouds are virtually symmetrical about the diagonal. The same is shown by the coefficient of determination R^2 values, which the graphs of the figures also show. While R^2 has a high value in the case of the mean load (the points lye close to the diagonal) the more spread out data in rest of the plots do not indicate any set-depended correlation in the data R^2 (very low R^2).

Different gray-scale levels in graphs of Figures 6a-c indicate the process stage from where the data point is from. Lightest color stands for the early process stage (small L) and the black color denotes the final stage (L = 250 m). Gray-scale levels in the figure demonstrate that mean, standard deviation and maximum (of concurrent load values) tend to be increase throughout the simulations. Plots in Figure 6c also demonstrate the earlier finding (Kujala et al., 2009; Suominen and Kujala, 2014; Ranta et al., 2017a) on the variation in the data increasing with the increasing load values. This is indicated by the wider spread in the cloud of data points for maximum load with the high than with the low maximum load values.

CONCLUSIONS

We performed 2D combined finite-discrete element method (FEM-DEM) simulations on ice-structure interaction process for studying the reasons behind the stochasticity of ice loads. The study based on three sets of 50 simulations, two sets with homogenous ice and one with nonhomogeneous ice. No clear set-dependency was found. In all of the cases load values were stochastic throughout the process. The stochastic nature of ice loads can be thus partly due to non-homogeneity of sea ice, but it can as well arise from the ice-structure interaction process itself; The ice-structure interaction process is itself a stochastic process. Understanding the sources for the stochasticity can be used to increase the accuracy of ice load estimates.

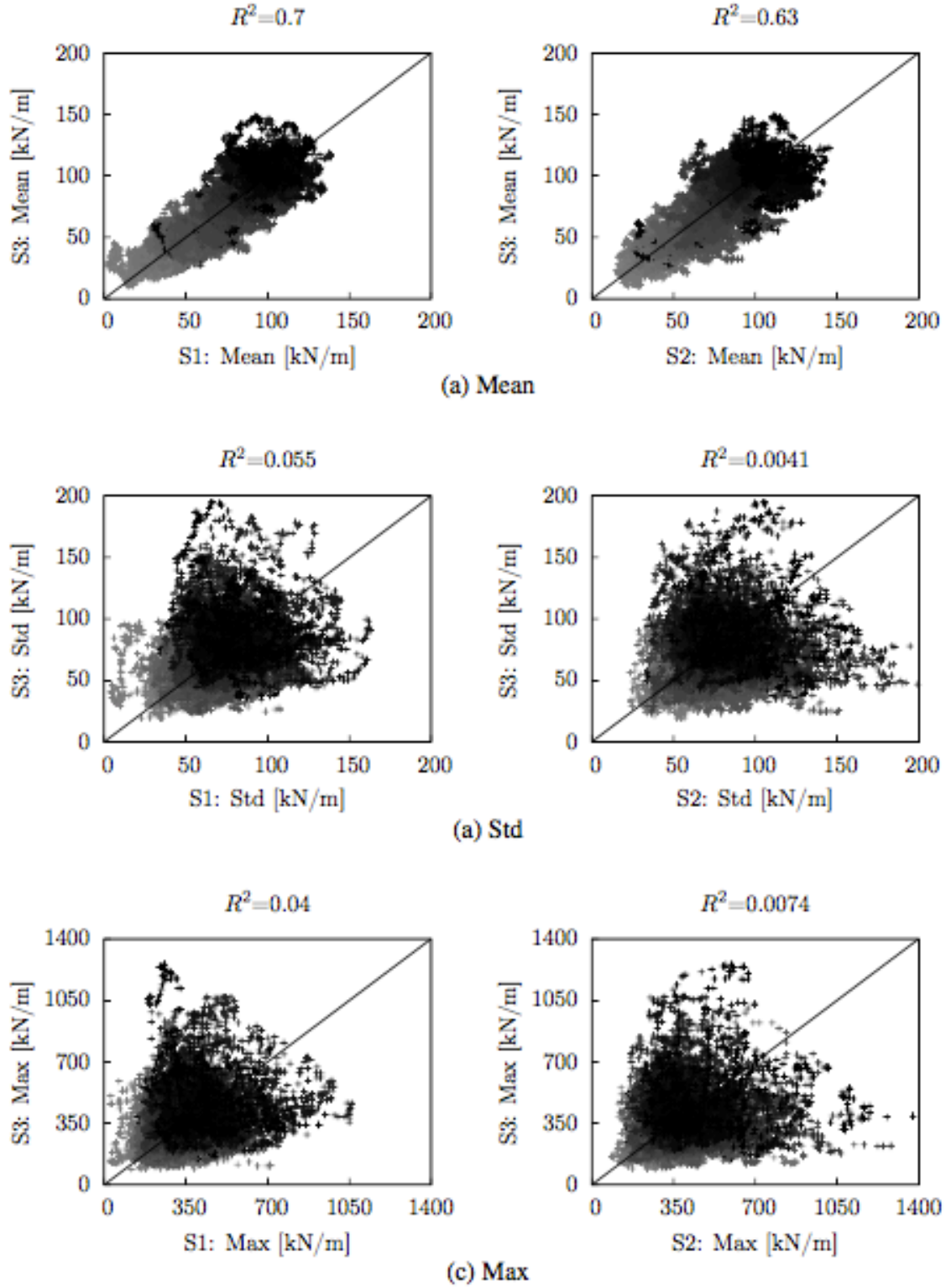

Figure 6: Comparison of concurrent mean (a), standard deviation (b) and maximum (c) load observations between simulations sets 1 and 2 (left column) and between simulation sets 2 and 3 (right column). Coefficients of determination R^2 are shown with 2 significant digits. Lightest colors stand for the early process stage (small L) and the black color the final stage (L = 250 m).

ACKNOWLEDGEMENTS

The authors wish to acknowledge the support from the Research Council of Norway through the Centre for Research-based Innovation SAMCoT and the support from all SAMCoT partners. Also the financial support from the Finnish Academy through research project Discrete Numerical Simulation and Statistical Analysis of the Failure Process of a Non-Homogenous Ice Sheet Against an Offshore Structure (DICE) is acknowledged.

REFERENCES

Daley, C., Tuhkuri, J., and Riska, K. (1998). The role of discrete failures in local ice loads. *Cold Regions Science and Technology*, 27(3):197 – 211.

Hopkins, M. (1992). Numerical simulation of systems of multitudinous polygonal blocks. Tech- nical Report 92-22, Cold Regions Research and Engineering Laboratory, CRREL. 69 p.

Jordaan, I. (2001). Mechanics of ice-structure interaction. *Engineering Fracture Mechanics*, 68:1923–1960.

Kujala, P., Suominen, M., and Riska, K. (2009). Statistics of ice loads measured on MT Uikku in the Baltic. In *Proceedings of the 20th International Conference on Port and Ocean Engineering under Arctic Conditions, POAC'09 (electronic publication)*.

Paavilainen, J. and Tuhkuri, J. (2012). Parameter effects on simulated ice rubbling forces on a wide sloping structure. *Cold Regions Science and Technology*, 81:1 – 10.

Paavilainen, J. and Tuhkuri, J. (2013). Pressure distributions and force chains during simulated ice rubbling against sloped structures. *Cold Regions Science and Technology*, 85:157 – 174.

Paavilainen, J., Tuhkuri, J., and Polojärvi, A. (2009). 2D combined finite–discrete element method to model multi-fracture of beam structures. *Engineering Computations*, 26(6):578–598.

Paavilainen, J., Tuhkuri, J., and Polojärvi, A. (2011). 2D numerical simulations of ice rubble formation process against an inclined structure. *Cold Regions Science and Technology*, 68(1-2):20–34.

Polojärvi, A., Pustogvar, A., and Tuhkuri, J. (2015). DEM simulations of direct shear box experiments of ice rubble: Force chains and peak loads. *Cold Regions Science and Technology*, 116:12–23.

Ranta, J., Polojärvi, A., and Tuhkuri, J. (2017a). The statistical analysis of peak ice loads in a simulated ice-structure interaction process. *Cold Regions Science and Technology*, 133:46– 55.

Ranta, J., Polojärvi, A., and Tuhkuri, J. (2017b). Statistics of peak loads in ice-structure interaction process: A study based on virtual experiments. *Submitted to Cold Regions Science and Technology*.

Suominen, M. and Kujala, P. (2014). Variation in short-term ice-induced load amplitudes on a ship's hull and related probability distributions. *Cold Regions Science and Technology*, 106-107:131–140.

Timco, G. and Weeks, W. (2010). A review of the engineering properties of sea ice. *Cold Regions Science and Technology*, 60(2):107–129.